◆ Human Brain Mapping 34:1768–1782 (2013) ◆

Brain Activity During Sympathetic Response in Anticipation and Experience of Pain

Frank Seifert,[1] Nadine Schuberth,[2] Roberto De Col,[2] Elena Peltz,[1] Florian T. Nickel,[1] and Christian Maihöfner[1,2]*

[1]*Department of Neurology, University Hospital Erlangen, Erlangen, Germany*
[2]*Department of Physiology and Pathophysiology, University of Erlangen-Nuremberg, Erlangen, Germany*

Abstract: Pain is a multidimensional phenomenon with sensory, affective, and autonomic components. Here, we used parametric functional magnetic resonance imaging (fMRI) to correlate regional brain activity with autonomic responses to (i) painful stimuli and to (ii) anticipation of pain. The autonomic parameters used for correlation were (i) skin blood flow (SBF) and (ii) skin conductance response (SCR). During (i) experience of pain and (ii) anticipation of pain, activity in the insular cortex, anterior cingulate cortex (ACC), prefrontal cortex (PFC), posterior parietal cortex (PPC), secondary somatosensory cortex (S2), thalamus, and midbrain correlated with sympathetic outflow. A conjunction analysis revealed a common central sympathetic network for (i) pain experience and (ii) pain anticipation with similar correlations between brain activity and sympathetic parameters in the anterior insula, prefrontal cortex, thalamus, midbrain, and temporoparietal junction. Therefore, we here describe shared central neural networks involved in the central autonomic processing of the experience and anticipation of pain. *Hum Brain Mapp 34:1768–1782, 2013.* © 2012 Wiley Periodicals, Inc.

Key words: pain; fMRI; autonomic nervous system; neuropathic pain; somatosensory system

INTRODUCTION

Pain is a multidimensional phenomenon with sensory, affective, and autonomic components. Painful stimuli activate a widespread neural network consisting of the primary (S1) and secondary somatosensory (S2) cortices, the insular cortex, the anterior cingulate cortex (ACC), the prefrontal cortices (PFC), thalamus, and brainstem nuclei [Apkarian et al., 2005; Tracey and Mantyh, 2007]. Many of these brain regions are also part of the central autonomic network [Benarroch, 2006; Saper, 2002]. Brain regions known to be involved in regulation of autonomic nervous system function are the ACC, the insular cortex, the amygdala, the hypothalamus, and, located in the brainstem, the periaqueductal gray (PAG), the parabrachial nucleus (PB), the nucleus of the solitary tract (NTS), the formatio reticularis, and the raphe nuclei [Benarroch, 2006]. As revealed by animal studies, there are close interactions between nociceptive and autonomic systems at all levels of the nervous system [Benarroch, 2006; Saper, 2002]. However, not much is known about pain-induced afferent and efferent autonomic processing in the central nervous system in humans. There, studies using neuroimaging techniques have identified the key roles of the dorsal anterior cingulate cortex (dACC), orbitofrontal cortex (OFC), and the anterior insular cortex in autonomic processing during mental or physical effort [Critchley, 2005]. In particular,

Frank Seifert and Nadine Schuberth contributed equally to this work.

Additional Supporting Information may be found in the online version of this article.

Contract grant sponsor: "German Research Network on Neuropathic Pain" (German Federal Ministry of Education and Research; BMBF); Contract grant sponsor: the German Research Foundation (KFO130).

*Correspondence to: Christian Maihöfner, Department of Neurology, University Hospital Erlangen, Schwabachanlage 6, D-91054 Erlangen, Germany. E-mail: christian.maihoefner@uk-erlangen.de

Received for publication 9 March 2011; Revised 19 October 2011; Accepted 5 December 2011

DOI: 10.1002/hbm.22035

Published online 22 March 2012 in Wiley Online Library (wileyonlinelibrary.com).

anterior cingulate cortex is implicated in generating autonomic changes, while insular cortex and OFC may be specialized in mapping visceral responses [Critchley, 2005]. Such a mapping of visceral responses is called interoception. Interoceptive stimuli that have been shown to activate the anterior insula are pain, itch, thirst, dyspnea, sensual touch, and heartbeat [Craig, 2009]. Critchley and colleagues found that in the right anterior insula neural activity and gray matter volume predict the participant's accuracy in a heartbeat detection task. Neuroanatomical data indicate that the lamina I spino-thalamo-cortical pathway, that conveys interoceptive and nociceptive information, projects to the viscerosensory cortex in the posterior and mid-insular cortices and is re-represented in the anterior part of the insula [Craig, 2002, 2003, 2009]. This re-representation is suggested to provide the basis for emotional awareness [Craig, 2002, 2003, 2009]. A few neuroimaging studies [Dube et al., 2009; Maihofner et al., 2010; Mobascher et al., 2009; Piche et al., 2010] have focused on brain activity in humans related to pain-induced autonomic activity. Brain activation associated with pain-related skin conductance reactivity was found in S1, S2, M1, insular cortex, ACC, PFC, amygdala, thalamus, and hypothalamus [Dube et al., 2009; Mobascher et al., 2009; Piche et al., 2010]. In a previous study using parametric fMRI and laser Doppler flowmetry we found increased activity in ACC, anterior insula and VLPFC and decreased activity of VMPFC, OFC, PCC, and occipital areas to be associated with pain-evoked sympathetic vasoconstrictor reflexes [Maihofner et al., 2010].

The biologic sense of pain is avoidance of tissue damage. Recognition of impeding pain leads to avoidance of noxious events and protects body integrity. However, there are experimental and clinical pain states where avoidance of pain is not possible. Then, anticipation of pain leads to autonomic arousal, anxiety, and increased pain intensity [Colloca et al., 2006; Ploghaus et al., 2001; Wise et al., 2007]. As revealed by fMRI, pain anticipation activates a cerebral network similar to the network activated by pain experience [Ploghaus et al., 1999], but with more anteriorly localized activity in medial prefrontal cortex and anterior insula. Anticipation of pain, like the experience of pain, is associated with autonomic responses. In the present study we used fMRI and an aversive conditioning paradigm to investigate brain activity correlating to autonomic nervous system activity during (i) anticipation and (ii) experience of pain. Thus, we correlated pain and pain anticipation induced changes in skin blood flow (SBF) and skin conductance response (SCR) to the MR signal time course. Skin vasoconstrictor responses and skin sudomotor responses at the fingertip closely parallel central sympathetic outflow [Janig and Habler, 2003; Wallin, 1990].

Previous studies investigating aversive conditioning have shown associated brain activity in the anterior cingulate, the anterior insula, the amygdala, and the hippocampus [Buchel et al., 1998, 1999]. However, to our knowledge, no study has investigated brain activity associated with sympathetic responses during pain anticipation.

METHODS

Participants

A total of 10 healthy participants participated in the study. One participant had to be excluded due to technical problems during the fMRI measurement. The remaining nine participants (six male, three female, mean age: 26.4 years $\pm$ 2.3 years) were included in the data analysis. All participants were right handed. The volunteers were informed about the procedures of the study. Informed consent was obtained from all participants before the experiments, and the study adhered to the tenets of the Declaration of Helsinki. The study was approved by the local ethics committee.

Experimental Design

We measured autonomic responses (changes in SBF and SCR) to pain experience and pain anticipation during fMRI. A block design with four conditions [(i) heat pain experience, (ii) innocuous warmth experience, (iii) heat pain anticipation, and (iv) innocuous warmth anticipation] was used. Preliminary tests (as described below in detail) were performed 2 weeks before the fMRI experiment to familiarize participants with the thermal stimuli and achieve a conditioning effect. The fMRI experiment started with an initial conditioning period, where we applied heat pain stimuli (heat pain experience) and innocuous warmth stimuli (innocuous warmth experience) simultaneously with colored lights (pain stimuli were paralleled by a red light; warmth stimuli were paralleled by a green light). After the conditioning period, in some of the stimulus blocks, only the light but no thermal stimulus was applied, resulting in stimulus anticipation (heat pain experience during red light, innocuous warmth experience during green light) (Fig. 1A). The sequence was the same in all participants. In parallel, we measured parameters of sympathetic outflow (SBF and SCR). Thus, we used an aversive conditioning paradigm where painful stimulation was the unconditioned stimulus (US) and changes in sympathetic outflow were the unconditioned response (UR). The displayed light was the conditioned stimulus (CS)—with red light as the excitatory conditioned stimulus (CS+) and green light as the inhibitory conditioned stimulus (CS−). Changes in sympathetic parameters were the conditioned responses (CR). Using parametric fMRI analysis we integrated both autonomic parameters into the fMRI design matrix and tried to determine those brain regions in which activity correlated with the sympathetic response to pain experience and pain anticipation [Maihofner et al., 2010].

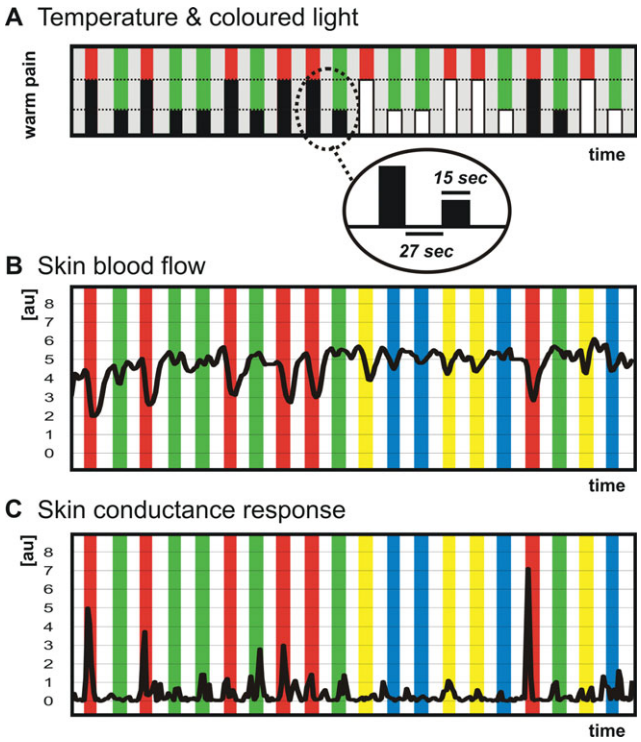

Figure 1.

Experimental procedure. **A**: Schematic diagram and time-line of the applied stimuli. Visually displayed colored lights signaled the heat pain (red light) and the innocuous warmth (green light) stimuli. After conditioning, only the light was displayed, but no thermal stimulus was applied (indicated by white boxes). **B**: The mean SBF during the experiment is shown: heat pain experience (red bars), warmth experience (green bars), heat pain anticipation (yellow bars), and warmth anticipation (blue bars). **C**: The mean skin conduction response during the experiment is shown: heat pain experience (red bars), warmth experience (green bars), heat pain anticipation (yellow bars), and warmth anticipation (blue bars). [Color figure can be viewed in the online issue, which is available at wileyonlinelibrary.com.]

Stimulus Application During the fMRI Measurement

The stimulation site in all participants was the left volar forearm. The thermal stimuli were applied using a peltier driven thermotest device with an fMRI suitable thermode (probe size 3 × 3 cm; TSA-II NeuroSensory Analyzer, Medoc Advanced Medical Systems, Rimat Yishai, Israel). The probe was placed on the skin and fixed with a rubber band. The stimuli were always applied at the same site. The baseline temperature of the thermode was 32°C. The individual heat pain threshold was determined using the method of limits [Yarnitsky and Sprecher, 1994] by taking the average of five successive heat stimuli. To determine the heat pain threshold the temperature stimuli were applied with a slope of 1°C/s. Subsequently, the participant was transferred into the MR scanner. During fMRI two different stimuli (heat pain and innocuous warmth stimulation) were applied in a pseudorandomized sequence (Fig. 1A). The slope for the temperature stimulation blocks was 4°/s. Heat pain stimulation was performed 1.5°C above the individual heat pain threshold. Innocuous warmth stimulation was performed 1.5°C below the individual heat pain threshold. The mean stimulus temperature for heat pain was 46.7 ± 0.4°C, and the mean stimulus temperature for innocuous warmth was 43.5 ± 0.5°C. Each stimulation block lasted 15 s, interrupted by a baseline of 27 s. Visually presented colored lights applied by a diode signaled the heat pain (red light) and the innocuous warmth (green light) stimuli. After conditioning (five stimulus blocks with heat pain and red light and five stimulus blocks with innocuous warmth and green light) only the light was displayed, but in some of the blocks (not all) there was no thermal stimulation (Fig. 1A). Altogether six stimulation blocks were applied for each stimulus type, that is, heat pain stimulation and innocuous warmth stimulation. Four blocks were applied for pain anticipation and warmth anticipation. After the fMRI measurement, participants had to rate the pain intensity of the heat pain stimuli and the warmth stimuli on an 11-point numerical pain rating scale ranging from 0 (no pain) to 10 (maximum pain). The MRI-scanner was inside an air-conditioned room in which the temperature was kept between 21 and 23°C. Participants had to acclimatize inside the room for at least 25 min. Furthermore, using an infrared thermometer it was guaranteed that the temperature at the index finger was not below 30°C. When necessary, the arm and trunk of the participants were covered by woolen blankets until a stable temperature situation at the hand had been achieved.

Two weeks before the fMRI experiment, the experiment was performed in a modified manner outside the MRI scanner to first familiarize participants with the thermal stimuli and achieve a conditioning effect. During those preliminary measurements, heat stimuli (simultaneously with red light) and warmth stimuli (simultaneously with green light) were applied in the same way as during the fMRI experiment. However, the conditions with pain anticipation and warmth anticipation were not included in the preliminary measurement.

Measurement of Skin Perfusion as a Marker for Sympathetic Activity

Skin blood flow (SBF) in the glabrous skin (of the left index finger) was measured during fMRI experiments using an MRI-suitable laser Doppler flowmeter (LDI, Moore Instruments, UK) as described in detail previously [Maihofner et al., 2010] (Fig. 1B). The fingertip was selected for investigation because it is known that the abundant arteriovenous anastomoses of this area are under strict sympathetic vasoconstrictor control [Janig and

Habler, 2003; Wallin, 1990]. During all experiments, laser Doppler signals were recorded online (IBM-compatible computer) using an analogue digital converter (Moore Instruments, UK), along with custom-made data acquisition software [Maihofner et al., 2010] for subsequent analysis. The sampling rate was 10 Hz, as was used in a previous parametric fMRI study [Maihofner et al., 2010]. Such a sampling rate is known to asses reliable values [Maihofner et al., 2010]. For SBF data no band-pass filter was applied [Maihofner et al., 2010]. Skin blood flow is expressed in arbitrary perfusion units [Maihofner et al., 2010; Wasner et al., 1999]. The SBF values were normalized and inverted by setting the baseline blood flow to a value of "0" and the maximal individual decrease in blood flow to a value of "1." This procedure allowed us to present the corresponding evoked vasoconstrictor responses as signal changes relative to the baseline flux and to implement these values into the fMRI design matrix. Data were baseline corrected using a running mean, and periods of 3 s were averaged to account for the repetition time of fMRI experiments [Maihofner et al., 2010].

Measurement of Electrodermal Activity as a Marker for Sympathetic Activity

Skin conductance responses (SCR) in the glabrous skin (of left fourth and fifth finger) were measured during fMRI experiments using an custom-made MRI-suitable SCR monitoring system as described by [Shastri et al., 2001] (Fig. 1C). During all experiments, SCR signals were recorded online (IBM-compatible computer), using an analogue digital converter (Moore Instruments, UK), along with custom-made data acquisition software [Maihofner et al., 2006a] for subsequent analysis. The sampling rate was 10 Hz. For SCR data a low-pass filter with a cut-off frequency of 1 Hz was applied as described previously [Shastri et al., 2001]. The baseline conductance was set at a value of "0," and corresponding SCR are presented as signal changes relative to the baseline conductance. Data were baseline corrected using a running mean, and periods of 3 s were averaged to account for the repetition time of fMRI experiments.

Functional Magnetic Resonance Imaging (fMRI)

Echoplanar images were collected on a 1.5 Tesla MRI scanner (Sonata, Siemens Medical Solutions, Erlangen, Germany) using the standard head coil. A total of 292 whole brain images were obtained with a gradient-echo, echo-planar scanning sequence (EPI; TR 3 s, time to echo 40 ms, flip angle 90°; field of view 220 mm^2, acquisition matrix 64 × 64, 16 axial slices, slice thickness 4 mm, gap 1 mm). The first three images were discarded to account for spin saturation effects, which resulted in 289 remaining images used for fMRI analysis. A three-dimensional, magnetization-prepared, rapid acquisition gradient echo sequence (MPRAGE) scan (voxel size = 1.0 × 1.0 × 1.0 mm^3) was recorded in the same session as the functional measurements for the recording of the individual brain anatomy. During each of the two sessions MRI sequences were assessed in the following order: anatomical scout, MPRAGE, EPI. Data analysis, registration, and visualization were performed with the fMRI software package Brainvoyager QX Version 1.1 as described previously [Maihofner et al., 2010; Peltz et al., 2010; Seifert et al., 2010] (www.brainvoyager.com). Data were motion-corrected using sinc interpolation. Preprocessing also included Gaussian spatial (FWHM = 4 mm) and temporal (FWHM = 3 volumes) smoothing of the functional data. Afterwards, the functional data were transformed into a standard stereotactic space and linear-interpolated to 3 × 3 × 3 mm [Talairach and Tournoux, 1988].

First, a block design was applied with each block lasting 15 s and five images being acquired. Each stimulation protocol served to obtain appropriate reference functions reflecting experimental and baseline conditions (stimulus = 1, baseline condition = 0). The reference functions served as independent predictors for a general linear model (GLM). Group analysis was performed resulting in T-statistical activation maps for the conditions (i) heat pain, (ii) anticipation of heat pain, (iii) warmth, and (iv) anticipation of warmth. For the activation maps, a threshold of $P < 0.0001$ (two-tailed, uncorrected for imaging purposes) and $T > 4$ was used. Bonferroni correction was performed at the cluster level. A minimum cluster size of 108 mm^3 was applied.

Second, a parametric fMRI analysis was performed. We implemented the evoked patterns of (i) sympathetically mediated vasoconstriction (SBF) and (ii) skin conductance response (SCR) as recorded online during fMRI (see above) as predictors in the GLM. This was then used to identify brain regions covarying with sympathetic activity. Thus, there were two groups of design matrices—one for SBF and one for SCR—and the result was two group parametric fMRI contrast maps. Parametric fMRI contrast maps (pain experience—warmth experience; and pain anticipation—warmth anticipation) were thresholded at $P < 0.01$ (FDR corrected). A minimum cluster size of 108 mm^3 was applied.

Furthermore, two conjunction analyses were performed to delineate those areas with similar correlation between brain activity and autonomic parameters (SBF and SCR) during pain experience and pain anticipation. The conjunction maps were thresholded at $P < 0.05$ (FDR corrected).

Statistical Analysis

Psychophysical data are presented as mean ± SEM. Statistical evaluation was performed using the STATISTICA software package. To assess statistically significant differences between autonomic responses a two-way repeated measures ANOVA (factors: condition and time) with post hoc Bonferroni test was used. P values <0.05 were considered as statistically significant.

RESULTS

Psychophysical Data

The heat pain stimuli were rated as 6.1 ± 0.4 (numerical rating scale for pain ranging from 0 to 10). The warmth stimuli were rated as 0.4 ± 0.2 (numerical rating scale for pain ranging from 0 to 10). Thus, as intended by the study design, heat pain stimuli but not warmth stimuli were painful.

Autonomic Measurements

We measured SBF and SCR during (i) heat pain stimulation, (ii) innocuous warmth stimulation, (iii) anticipation of heat pain, and (iv) anticipation of innocuous warmth. Figure 2 shows the time course of the mean SBF (Fig. 2A) and SCR (Fig. 2B) during each tested condition. There was a significant reduction in SBF during pain experience ($P < 0.05$, ANOVA, Bonferroni corrected) and during pain anticipation ($P < 0.05$, ANOVA, Bonferroni corrected). During warmth and warmth anticipation, there was no significant change in SBF ($P > 0.05$, ANOVA, Bonferroni corrected). The vasoconstrictor response was significantly stronger during pain experience than during the other conditions ($P < 0.05$, ANOVA, Bonferroni corrected). We found a significant reduction in skin resistance during pain experience ($P < 0.05$, ANOVA, Bonferroni corrected). During pain anticipation, warmth, and warmth anticipation, there was no significant change in skin resistance ($P > 0.05$, ANOVA, Bonferroni corrected). The sympathetic skin response was significantly stronger during pain experience than during the other conditions ($P < 0.05$, ANOVA, Bonferroni corrected).

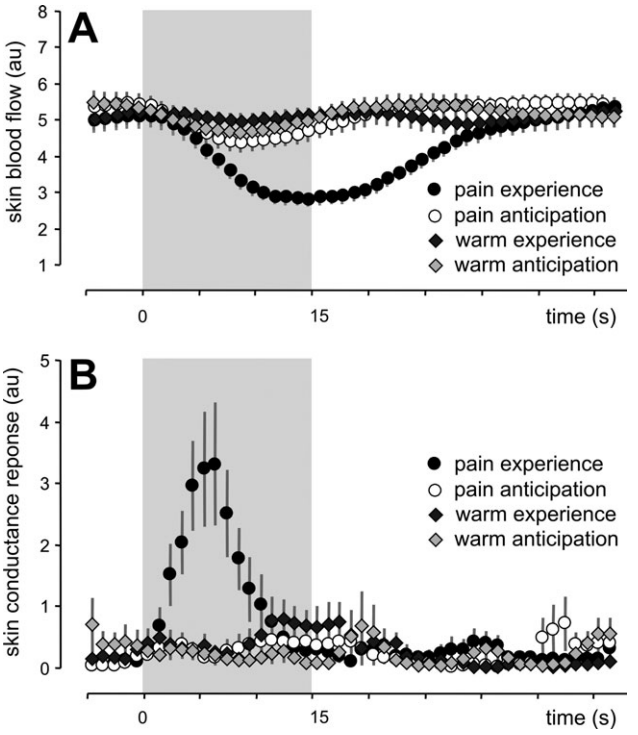

Figure 2.
A: Skin blood flow during all tested conditions. **B**: Skin resistance during all tested conditions. Means ± SEM.

Cerebral Activations Induced by Stimulus Experience and Stimulus Anticipation: Block Design

Functional magnetic resonance imaging analysis revealed brain areas activated by (i) heat pain stimulation, (ii) innocuous warmth stimulation, (iii), anticipation of heat pain, and (iv) anticipation of innocuous warmth. During (i) the experience of pain, activity was detected in the bilateral secondary somatosensory cortex (S2), bilateral anterior and posterior insular cortices, anterior cingulate cortex (ACC), bilateral dorsolateral and ventrolateral prefrontal cortices (DLPFC and VLPFC), contralateral medial prefrontal cortex (MPFC), ipsilateral premotor cortex (PMC), bilateral basal ganglia, bilateral thalamus, and bilateral cerebellum (coded red–yellow in Supporting Information Fig. S1A). Deactivations were seen in the bilateral subgenual ACC, the contralateral VLPFC, ipsilateral M1, and ipsilateral temporal cortex (coded blue–green in Supporting Information Fig. S1A). During (ii) anticipation of pain, activity was found in anterior operculum, anterior insular cortex, bilateral MPFC/ ACC, bilateral DLPFC, bilateral VPFC, ipsilateral VLPFC, bilateral dorsal prefrontal cortex (DPFC), bilateral PMC, contralateral temporal cortex, bilateral supramarginal gyrus, contralateral occipital cortex, bilateral thalamus, and bilateral cerebellum (coded red–yellow in Supporting Information Fig. S1B). Deactivation was found in bilateral S1 and ipsilateral subgenual ACC (coded blue–green in Supporting Information Fig. S1B). During (iii) warmth experience, activity in the bilateral anterior insular cortex, bilateral DLPFC, contralateral VPFC and VLPFC, ipsilateral basal ganglia, bilateral occipital cortex, and bilateral cerebellum was detected (coded red–yellow in Supporting Information Fig. S1C). During (iv) anticipation of innocuous warmth, activity was detected in bilateral anterior insular cortex, contralateral posterior insular cortex, contralateral DLPFC, ipsilateral VLPFC, ipsilateral VPFC and DPFC, contralateral M1, bilateral IPL, ipsilateral supramarginal gyrus, bilateral temporal cortex, contralateral occipital cortex, and bilateral cerebellum (coded red–yellow in Supporting Information Fig. S1D).

Cerebral Activation Correlated to Autonomic Responses: Parametric Analysis

In a next step, we introduced sympathetic vasoconstrictor patterns (SBF) and skin conductance response (SCR) as

predictors for the GLM. Brain activity correlating positively with (i) SBF during pain experience was detected in contralateral S2, contralateral anterior and posterior insula, bilateral ACC, bilateral DLPFC, ipsilateral MPFC, contralateral SMA, bilateral PMC, ipsilateral M1, bilateral PPC, temporoparietal junction, occipital cortex, ipsilateral thalamus, and ipsilateral midbrain (Fig. 3A, coded red–yellow; Table I). Negative correlations were also detected. Areas with negative correlations between BOLD-signal and SBF are presented in Table I and Supporting Information Figure S2A. Cerebral activity correlating positively with (ii) SBF during pain anticipation was detected in ipsilateral S2, ipsilateral anterior and posterior insula, bilateral ACC, contralateral posterior cingulate cortex (PCC), ipsilateral DLPFC, contralateral VLPFC, contralateral MPFC, ipsilateral PMC, ipsilateral M1, bilateral PPC, ipsilateral temporal cortex, hippocampus, bilateral basal ganglia, and contralateral midbrain (Fig. 3B, coded red–yellow; Table I). Negative correlations were also detected. Areas with negative correlations between BOLD-signal and SBF are presented in Table I and Supporting Information Figure S2B. Brain activity correlating with (iii) SCR during pain experience was detected in contralateral S2, bilateral anterior insula, bilateral ACC, bilateral middle cingulate gyrus, bilateral DLPFC, ipsilateral MPFC, bilateral PMC, contralateral PPC, ipsilateral IPL, temporal and occipital cortex, contralateral basal ganglia, ipsilateral thalamus, and ipsilateral midbrain (Fig. 3C, coded red–yellow; Table I). Negative correlations were also detected. Areas with negative correlations between BOLD-signal and SCR are presented in Table I and Supporting Information Figure S2C. Brain activity correlating with (iv) SCR during pain anticipation was detected in ipsilateral anterior insula, bilateral ACC, bilateral DLPFC, bilateral MPFC, contralateral SMA, bilateral PMC, bilateral PPC, contralateral supramarginal gyrus, contralateral hippocampus, occipital and temporal cortex, bilateral basal ganglia, and ipsilateral thalamus (Fig. 3D, coded red–yellow; Table I). Negative correlations were also detected. Areas with negative correlations between BOLD-signal and SCR are presented in Table I and Supporting Information Figure S2D.

Furthermore, two conjunction analyses were performed to delineate those areas with similar correlations between brain activity and autonomic parameters (SBF and SCR) during the experience and anticipation of pain. The first conjunction analysis revealed those areas with similar correlations between neural activity and SBF during pain experience and anticipation. This shared network consists of bilateral dorsolateral and ventrolateral PFC, medial PFC, thalamus, midbrain, and areas of the temporoparietal junction (Fig. 4A, coded red–yellow; Table II). The second conjunction analysis revealed those areas with similar correlations between neural activity and SCR during pain experience and anticipation. This network consists of the anterior insula, bilateral dorsolateral and ventrolateral PFC, thalamus, midbrain, and areas in the temporoparietal junction (Fig. 4B, coded red–yellow; Table II).

DISCUSSION

The cerebral processes involved in autonomic processing of pain anticipation have not been investigated until now. Therefore, we used functional magnetic resonance imaging (fMRI) to correlate sympathetic responses to (i) pain experience and (ii) pain anticipation with regional brain activity. We here describe a shared central neural network involved in the sympathetic response to the experience and anticipation of pain.

When fMRI data were analyzed in a conventional block design, known brain networks for pain experience and pain anticipation were activated. Heat pain activated the anterior and posterior insula, ACC, PFC, S2, thalamus, basal ganglia, and cerebellum, which is consistent with existing literature [Apkarian et al., 2005; Seifert and Maihofner, 2009; Tracey and Mantyh, 2007; Treede et al., 1999]. Innocuous warmth activated the anterior insula, PFC, and cerebellum as has already been described for warmth stimulation [Peltz et al., 2010; Tseng et al., 2010]. We found that the network activated during pain anticipation was similar to the one activated during pain experience. This is also a finding which has already been reported [Ploghaus et al., 1999; Porro et al., 2002]. Also consistent with previous literature [Ploghaus et al., 1999], we observed activity in MPFC/ACC (ipsilateral $y = 33$ vs. $y = 11$, contralateral $y = 38$ vs. $y = 8$) and insular cortex (ipsilateral $y = 21$ vs. $y = 11$, contralateral $y = 22$ vs. $y = 11$), located more rostrally (Supporting Information Fig. S1C).

Common Central Sympathetic Networks for Pain Experience and Anticipation

To determine those brain regions where activity is associated with sympathetic nervous system activity, we measured the sympathetic vasoconstrictor reflex (skin blood flow, SBF) and skin conductance response (SCR) induced by pain and pain anticipation during the fMRI measurements. We then implemented the individual measurements of SBF and SCR into the fMRI design matrix to correlate regional brain activity with sympathetic activity. Interestingly, both during (i) the experience of pain and (ii) anticipation of pain, activity in the insular cortex, ACC, PFC, PPC, S2, thalamus, and midbrain correlated with parameters of sympathetic outflow. Furthermore, a conjunction analysis revealed a common central sympathetic network for pain experience and pain anticipation. Similar correlations between brain activity and sympathetic parameters were detected in the anterior insula, prefrontal cortex (MPFC, VLPFC, and DLPFC), thalamus, midbrain, and in the contralateral temporoparietal junction. This demonstrates that shared central neural networks are involved in the central autonomic processing of the experience and anticipation of pain. Therefore, in the following we will discuss those brain regions in detail, where brain activity correlated with parameters of sympathetic response.

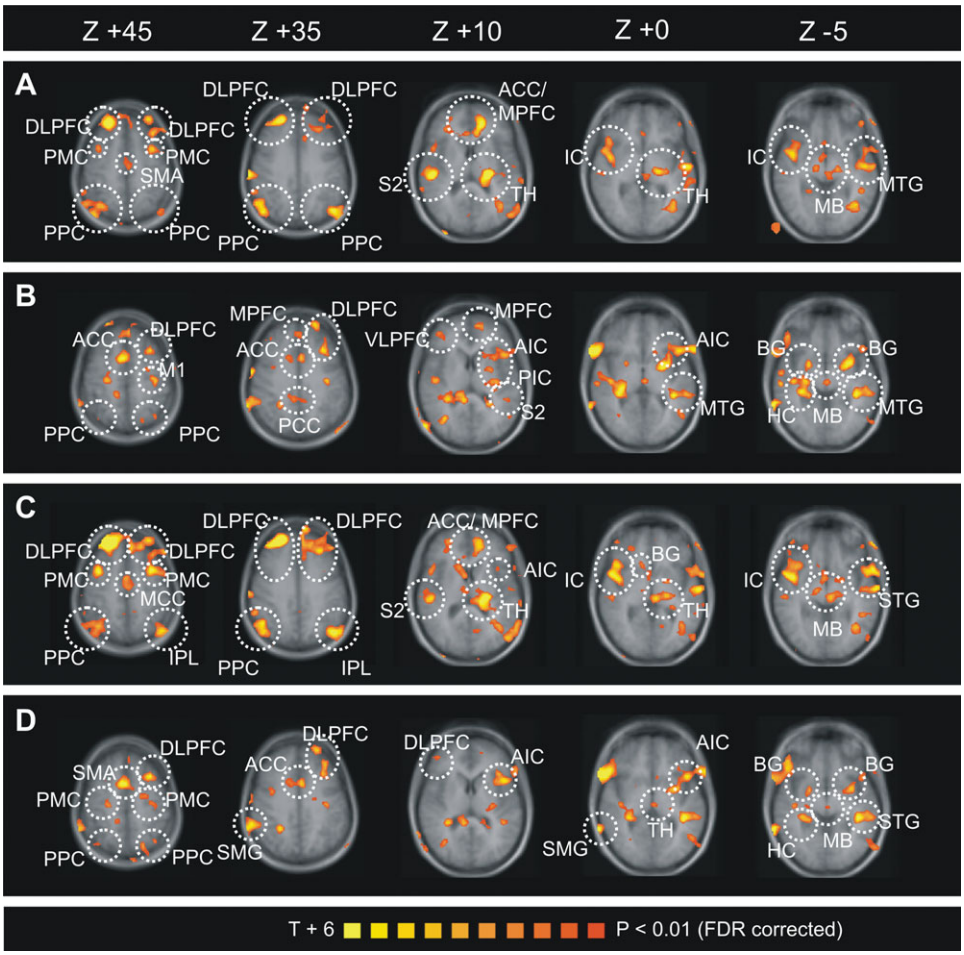

Figure 3.

Parametrical fMRI analysis. The *T*-statistic contrast map shows areas with activity covarying with autonomic response: (**A**) SBF and heat pain (heat pain–warmth), (**B**) SBF and anticipation of heat pain (pain anticipation–anticipation of warmth), (**C**) SCR and heat pain (heat pain–warmth), (**D**) SCR and anticipation of pain (pain anticipation–anticipation of warmth). The group statistic contrast maps are registered onto the averaged Talairach-transformed brains, thresholded at $P < 0.01$ (FDR corrected). The Talairach-coordinates and cluster sizes are depicted in Table I. Left hemisphere—ipsilateral; right hemisphere—contralateral. ACC, anterior cingulate cortex; MPFC, medial prefrontal cortex; DLPFC, dorsolateral prefrontal cortex; VLPFC, ventrolateral prefrontal cortex; IC, insular cortex; AIC, anterior insular cortex; PIC, posterior insular cortex; S2, secondary somatosensory cortex; PPC, posterior parietal cortex; M1, primary motor cortex; PMC; premotor cortex; MTG, middle temporal gyrus; STG, superior temporal gyrus; IPL, inferior parietal lobule; HC, hippocampus; BG, basal ganglia; TH, thalamus; MB, midbrain. [Color figure can be viewed in the online issue, which is available at wileyonlinelibrary.com.]

Insular Cortex

The insula is a central representation site for pain, pain anticipation, emotion, and interoception [Brooks and Tracey, 2007; Craig, 2002, 2003; Critchley et al., 2004; Ploghaus et al., 1999; Porro et al., 2002; Tracey and Mantyh, 2007]. The lamina I spino-thalamo-cortical pathway, that conveys interoceptive and nociceptive information, projects to the viscerosensory cortex in the mid insula [Leone et al., 2006] and is re-represented in the anterior part of the insular cortex [Craig, 2002, 2003]. This re-representation may provide the basis for emotional awareness [Craig, 2002, 2003]. Thus, for interoception (and pain as a significant interoceptive feeling), a distinction between the anterior and posterior insula must be made. In humans, the posterior insula seems to receive direct nociceptive and thermoceptive input from the thalamus via the lamina I spino-thalamo-cortical pathway [Craig, 2002, 2003, 2009]. This information is then integrated with other input in the anterior insula [Craig, 2002, 2003, 2009]. By using PET it was demonstrated that temperature stimuli are represented linearly in the contralateral posterior insula, whereas subjective ratings of these stimuli correlate with

TABLE I. Parametric fMRI analysis

Region	Side	*X*	*Y*	*Z*	BA	*t*-score	*P*-value (corr.)	Size (mm^3)
(a) Skin blood flow—Pain experience (contrasted with warmth experience)								
Positive correlation								
S2	Contra	56	−21	18	40	6.442	0.000001	7,796
AIC	Contra	44	12	−1	13	3.758	0.000175	4,616
PIC	Contra	42	−2	0	13	3.355	0.000805	1,801
ACC	Ipsi	−12	32	22	32	6.062	0.000001	8,293
ACC	Contra	5	30	7	24	3.207	0.000001	441
DLPFC	Ipsi	−29	43	30	9	5.476	0.000001	6,671
DLPFC	Contra	22	44	43	8	6.149	0.000001	10,709
MPFC	Ipsi	−13	47	21	9	5.483	0.000001	7,806
SMA	Contra	3	−15	53	6	5.488	0.000001	2,451
PMC	Ipsi	−30	4	59	6	7.279	0,000001	12,404
PMC	Contra	24	7	59	6	6.428	0.000001	10,203
M1	Ipsi	−30	−24	57	4	3.340	0.000849	134
PPC	Contra	32	−62	52	7	8.295	0.000001	17,189
PPC	Ipsi	−18	−75	56	7	5.592	0.000001	1,728
IPL	Contra	47	−60	38	40	6.808	0.000001	10,434
Angular. gy.	Ipsi	−47	−69	35	39	3.542	0.000404	4,613
Cuneus	Ipsi	−5	−73	21	18	4.601	0.000004	1,959
Mid. temp. gy	Ipsi	−53	−20	−1	21	5.528	0.000001	6,648
Parahipp. gy	Contra	22	−44	−8	36	3.376	0.000746	567
Thalamus	Ipsi	−18	−24	7	–	5.975	0.000001	7,145
Midbrain	Ipsi	−6	−24	−10	–	5.007	0.000001	5,809
Negative correlation								
S1	Ipsi	−16	−38	58	3	−7.204	0.000001	8,711
IC	Ipsi	−36	−3	17	13	−3.626	0.000293	1,087
ACC	Contra	13	17	39	32	−5.186	0.000001	6,033
MCC	Ipsi	−17	−13	35	24	−6.418	0.000001	5,835
MCC	Contra	13	−17	33	24	−8.074	0.000001	6,886
MPFC	Contra	5	64	26	10	−3.887	0.000104	2,182
MPFC	Contra	12	49	−1	10	−6.051	0.000001	4,416
IPL	Ipsi	−38	−36	41	40	−7.062	0.000001	23,886
Fusiform gy.	Ipsi	−19	−86	−12	18	−6.152	0.000001	25,339
Lingual gy.	Contra	22	−75	−6	18	−6.137	0.000001	46,448
Cerebellum	Ipsi	−16	−51	−40	–	−3.930	0.000087	206
Cerebellum	Contra	30	−40	−29	–	−8.201	0.000001	12,761
(b) Skin blood flow—Pain anticipation (contrasted with warmth anticipation)								
Positive correlation								
S2	Ipsi	−53	−23	21	40	3.121	0.001826	122
AIC	Ipsi	−38	15	2	13	5.985	0.000001	11,745
PIC	Ipsi	−31	−19	15	13	5.412	0.000001	3,615
ACC	Ipsi	−2	13	38	32	3.715	0.000208	1,197
ACC	Contra	9	13	40	32	5.809	0.000001	2,141
PCC	Contra	9	−37	39	31	3.771	0.000167	1,735
DLPFC	Ipsi	−20	51	30	9	4.547	0.000006	3,869
VLPFC	Contra	38	42	21	10	3.288	0.001023	4,142
MPFC	Contra	1	41	46	8	5.169	0.000001	4,606
PMC	Ipsi	−26	17	51	6	4.493	0.000007	5,817
M1	Ipsi	−34	−17	44	4	5.420	0.000001	3,079
PPC	Ipsi	−35	−62	44	7	3.511	0.000455	247

TABLE I. (Continued)

Positive correlation								
PPC	Contra	32	−41	57	5	4.760	0.000002	1,288
Mid. temp. gy	Ipsi	−45	−34	−2	21	3.472	0.000526	4,411
Hippocampus	Contra	30	−29	0	–	5.775	0.000001	9,888
Basal ganglia	Ipsi	−26	3	−1	–	6.408	0.000001	4,661
Basal ganglia	Contra	22	2	−6	–	4.626	0.000004	1,289
Midbrain	Contra	−2	−19	−1	–	3.069	0.002171	662
Negative correlation								
S1	Ipsi	−20	−32	65	3	−6.7723	0.000001	3,947
S1	Contra	13	−33	67	3	−5.788	0.000001	4,341
AIC	Contra	33	16	6	13	−3.724	0.000187	1,315
PIC	Contra	32	−18	18	13	−3.306	0.000961	590
VPFC	Ipsi	−28	53	−3	10	−5.296	0.000001	6,906
MPFC	Ipsi	−19	30	31	9	−5.216	0.000001	1,844
MPFC	Contra	12	56	17	10	−6.616	0.000001	14,350
STG	Ipsi	−54	−9	−4	22	−7.649	0.000001	13,593
STG	Contra	59	−36	11	22	−5.007	0.000001	2,799
Cuneus	Ipsi	−18	−79	26	18	−5.394	0.000001	6,696
Cuneus	Contra	14	−76	32	19	−5.183	0.000001	10,906
Thalamus	Contra	10	−6	2	–	−3.108	0.001906	359
Cerebellum	Ipsi	−43	−55	−40	–	−2.957	0.003135	181
Cerebellum	Contra	42	−42	−36	–	−4.111	0.000041	1,047
(c) Skin conductance response—Pain experience contrasted with warmth experience								
Positive correlation								
S2	Contra	57	−21	16	40	4.990	0.000001	5,762
AIC	Ipsi	−37	14	10	13	3.479	0.000511	201
AIC	Contra	46	10	−3	13	4.006	0.000064	9,085
ACC	Ipsi	−11	30	25	32	4.598	0.000004	6,309
ACC	Contra	5	30	7	24	3.237	0.001223	210
MCC	Ipsi	−5	−7	43	24	4.385	0.000012	706
MCC	Contra	1	−4	46	24	4.947	0.000001	1,611
DLPFC	Ipsi	−26	41	34	9	5.505	0.000001	19,005
DLPFC	Contra	23	43	41	8	6.439	0.000001	18,468
MPFC	Ipsi	−9	60	30	9	4.941	0.000001	2,476
PMC	Ipsi	−3	11	57	6	6.280	0.000001	19,718
PMC	Contra	26	10	56	6	5.974	0.000001	14,494
IPL	Ipsi	−48	−67	33	39	4.224	0.000025	12,932
PPC	Contra	36	−61	48	7	7.289	0.000001	19,258
Sup. temp.gy.	Ipsi	−57	−12	−2	21	4.547	0.000006	3,695
Fusifo. gy.	Ipsi	−37	−66	−11	19	5.208	0.000001	12,465
Subcallosal gy.	Ipsi	−13	2	−14	34	6.439	0.000001	4,867
Basal ganglia	Contra	11	14	5	–	5.223	0.000001	5,568
Thalamus	Ipsi	−15	−25	6	–	5.002	0.000001	10,921
Midbrain	Ipsi	−8	−22	−4	–	3.972	0.000073	1,988
Negative correlation								
ACC	Contra	19	13	39	32	−4.029	0.000058	4,069
DLPFC	Contra	51	9	26	9	−6.883	0.000001	6,814
MPFC	Contra	0	65	25	10	−4.724	0.000002	1,516
MPFC	Contra	9	40	29	9	−3.896	0.000100	856
IPL	Ipsi	−41	−37	41	40	−5.817	0.000001	16,998
IPL	Contra	33	−35	41	40	−5.165	0.000001	9,252
STG	Contra	41	−38	3	41	−4.837	0.000001	10,676
Lingual gy.	Ipsi	−20	−86	1	17	−5.372	0.000001	18,324

TABLE I. (Continued)

Lingual gy.	Contra	13	−81	−7	17	−4.040	0.000055	17,363
Parahippoc. gy.	Contra	24	−2	−13	–	−5.161	0.000001	6,250
Cerebellum	Ipsi	−16	−51	−39	–	−4.016	0.000061	245
Cerebellum	Contra	30	−40	−26	–	−7.350	0.000001	13,732
(d) Skin conductance response—Pain anticipation contrasted with warmth anticipation								
Positive correlation								
AIC	Ipsi	−39	16	8	13	4.730	0.000002	7,523
ACC	Ipsi	−2	11	41	32	4.100	0.000043	2,124
ACC	Contra	10	12	40	32	5.762	0.000001	2,511
DLPFC	Ipsi	−24	47	31	9	3.774	0.000164	3,970
DLPFC	Contra	44	35	22	46	5.594	0.000001	6,498
MPFC	Ipsi	−5	45	21	9	3.866	0.000114	645
MPFC	Contra	8	29	55	8	5.012	0.000001	1,314
SMA	Contra	12	6	55	6	4.891	0.000001	1,876
PMC	Ipsi	−26	20	51	6	4.862	0.000001	9,383
PMC	Contra	37	4	29	6	3.849	0.000122	1,668
PPC	Ipsi	−2	−72	52	7	5.363	0.000001	1,756
PPC	Contra	25	−68	55	7	5.163	0.000001	2,117
Sup. temp. gy.	Ipsi	−40	−30	3	41	4.382	0.000012	7,231
Supramrag. gy.	Contra	61	−46	31	40	7.037	0.000001	6,514
Hippocampus	Contra	31	−31	0	–	5.137	0.000001	4,563
Declive	Contra	13	−73	−14	–	4.433	0.000010	1,463
Basal ganglia	Ipsi	−29	2	−1	–	4.963	0.000001	2,683
Basal ganglia	Contra	23	0	−6	–	3.891	0.000102	650
Thalamus	Ipsi	−2	−19	0	–	2.234	0.020204	377
Negative correlation								
S1	Ipsi	−22	−31	66	3	−6.145	0.000001	3,941
S1	Contra	14	−35	67	3	−4.347	0.000014	1,948
M1	Contra	42	−16	45	4	−3.257	0.001142	773
DLPFC	Ipsi	−38	36	16	46	−3.005	0.002683	195
MPFC	Contra	8	60	19	10	−7.727	0.000001	13,076
IPL	Contra	44	−37	48	40	−2.807	0.005038	245
Lingual gy.	Ipsi	−11	−81	−5	18	−5.685	0.000001	24,026
Middle temp. gy.	Ipsi	−52	−12	−13	21	−5.556	0.000001	3,899
Sup. temp. gy.	Contra	56	−35	9	22	−4.251	0.000022	1,522
Fusif. gy.	Contra	41	−54	−13	37	−6.031	0.000001	8,300
Cerebellum	Ipsi	−6	−67	−34	–	−5.892	0.000001	5,613
Cerebellum	Contra	8	−54	−36	–	−6.410	0.000001	2,482

S2, secondary somatosensory cortex; AIC, anterior insular cortex; PIC, posterior insular cortex; ACC, anterior cingulate cortex; MPFC, medial prefrontal cortex; DLPFC, dorsolateral prefrontal cortex; VLPFC, ventrolateral prefrontal cortex; VPFC, ventral prefrontal cortex; DPFC, dorsal prefrontal cortex; SMA, supplementary motor cortex, PMC, premotor cortex, M1, primary motor cortex, PPC, posterior parietal cortex; IPL, inferior parietal lobulus; Contra, contralateral (right hemisphere); ipsi, ipsilateral (left hemisphere).

activity in mid-insular cortex and most strongly with activity in the right anterior insula and adjacent orbitofrontal cortex [Craig et al., 2000]. This posterior-to-mid-to-anterior pattern of integration of interoceptive information suggests that the anterior insula plays a fundamental role in human awareness, with a representation of all subjective feelings from the body [Craig, 2009]. Previous work found pain-related changes in peripheral sympathetic activity to be associated with brain activation in the insular cortex [Dube et al., 2009; Maihofner et al., 2010; Mobascher et al., 2009]. The insula was also found to be associated with the anticipation of pain [Ploghaus et al., 1999; Porro et al., 2002; Wise et al., 2007] and other aversive events [Buchel et al., 1998; Chua et al., 1999]. In the present study, we found that activity in the anterior insula correlated to both SBF and SCR during both pain experience and pain anticipation. Interestingly,

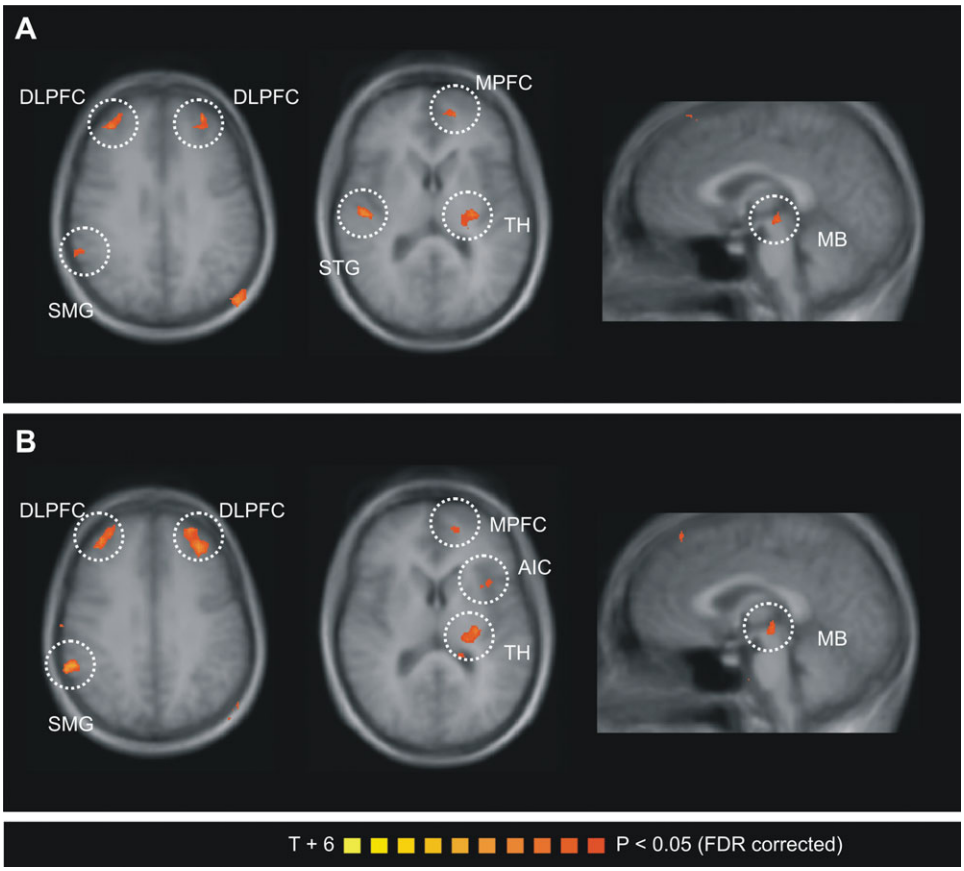

Figure 4.

Conjunction analysis of the parametrical fMRI data. The *T*-statistic conjunction map shows areas in which activity covaries with autonomic response similarly during pain experience and pain anticipation: (**A**) skin blood flow and (**B**) sympathetic skin response. The group statistic conjunction maps are registered onto the averaged Talairach-transformed brains, thresholded at $P < 0.05$ (FDR corrected). The Talairach-coordinates and cluster sizes are depicted in Table II. Left hemisphere—ipsilateral; right hemisphere—contralateral. MPFC, medial prefrontal cortex; DLPFC, dorsolateral prefrontal cortex; VLPFC, ventrolateral prefrontal cortex; AIC, anterior insular cortex; MTG, middle temporal gyrus; STG, superior temporal gyrus; TH, thalamus; MB, midbrain. [Color figure can be viewed in the online issue, which is available at wileyonlinelibrary.com.]

during pain anticipation, activity in the ipsilateral anterior insular cortex correlated with sympathetic parameters. However, during pain experience, significant correlation with autonomic parameters was found contralateral to the stimulation. Our results indicate a role in autonomic processing during both pain experience and pain anticipation.

Anterior Cingulate Cortex

The anterior cingulate cortex plays a major role in pain processing [Apkarian et al., 2005; Seifert and Maihofner, 2009] and pain anticipation [Ploghaus et al., 1999; Porro et al., 2002]. Activity within the dorsal ACC was found to be linked to autonomic cardiovascular control during mental or physical effort [Critchley et al., 2000a, 2001b, 2003], during reward anticipation [Critchley et al., 2001a], and during error cognition [Critchley et al., 2005]. Patients with ACC lesions showed a blunted autonomic arousal [Critchley et al., 2003]. Therefore, a role for the ACC in the generation of autonomic arousal has been suggested [Critchley, 2009]. In a previous study, our group demonstrated that ACC activity was correlated with pain-induced sympathetic vasoconstrictor responses [Maihofner et al., 2010]. Moreover, ACC activation was associated with heat-pain related skin conductance reactivity [Dube et al., 2009]. In our present study, we have demonstrated that activity within the ACC is correlated not only with pain-induced sympathetic vasoconstrictor reflexes and skin conductance response, but also with the sympathetic responses occurring during pain anticipation.

Prefrontal Cortex

We found activity in prefrontal cortex which correlated with SBF and SCR during pain and pain anticipation. The

TABLE II. Conjunction analysis

Region	Side	X	Y	Z	BA	Size (mm^3)
(a) Skin blood flow—Pain experience (contrasted with warmth experience) and pain anticipation (contrasted with warmth anticipation)						
Positive correlation						
DLPFC/VLPFC	Ipsi	−24	43	25	9/10	1,161
VLPFC	Contra	35	35	15	10	164
DLPFC	Contra	33	46	28	9	532
MPFC	Ipsi	−12	49	14	10	814
MPFC	Ipsi	−3	37	53	8	586
PMC	Ipsi	−23	6	66	6	1,637
SMG	Contra	57	−44	36	40	543
Middle temp. gy.	Ipsi	−56	−36	2	22	263
Middle temp gy.	Ipsi	−50	−76	28	39	1,172
Sup. temp. gy.	Contra	48	−17	9	22	529
Thalamus	Ipsi	−24	−21	9	–	915
Midbrain	Ipsi	−2	−21	−4	–	193
Negative correlation						
S1	Ipsi	−18	−35	57	3	1,355
MPFC	Contra	4	64	27	10	1,419
MPFC	Contra	14	50	2	10	2,206
DLPFC	Contra	48	5	34	9	389
IPL	Ipsi	−33	−40	31	40	3,796
Precuneus	Ipsi	−22	−73	27	31	399
Precuneus	Contra	16	−68	33	7	1,624
Cerebellum	Contra	29	−41	−25	–	1,971
(b) Skin conductance response—Pain experience (contrasted with warmth experience) and pain anticipation (contrasted with warmth anticipation)						
Positive correlation						
AIC	Ipsi	−35	13	11	13	138
DLPFC	Ipsi	−26	42	28	9	3,336
DLPFC	Contra	34	46	28	9	1,527
VLPFC	Contra	47	23	−1	47	584
MPFC	Ipsi	−16	45	18	9	1,426
PMC	Ipsi	−27	14	59	6	4,291
PMC	Contra	10	22	60	6	539
SMG/IPL	Contra	56	−44	36	40	1,039
SPL	Contra	27	−68	55	7	2,372
Middle temp. gy.	Ipsi	−49	−77	27	39	635
Sup. temp. gy.	Contra	47	1	−4	7	132
Precuneus	Ipsi	−20	−74	55	7	1,055
Basal ganglia	Ipsi	−21	−2	0	–	368
Thalamus	Ipsi	−23	−23	7	–	1,357
Midbrain	Ipsi	−2	−21	−2	–	255
Cerebellum	Contra	28	−51	−39	–	200
Negative correlation						
MPFC	Contra	4	64	29	10	3,036
MPFC	Contra	23	59	−4	10	3,625
IPL	Ipsi	−31	−39	37	40	6,453
Middle temp. gy.	Contra	55	−37	4	22	467
Precuneus	Contra	10	−70	36	7	3,927
Lingual gy.	Contra	−8	−84	0	17	7,270
Cerebellum	Contra	33	−41	−23	–	764

AIC, anterior insular cortex; MPFC, medial prefrontal cortex; DLPFC, dorsolateral prefrontal cortex; VLPFC, ventrolateral prefrontal cortex; PMC, premotor cortex, IPL, inferior parietal lobulus; SPL, superior parietal lobulus; SMG, supramarginal gyrus; Contra, contralateral (right hemisphere); ipsi, ipsilateral (left hemisphere).

MPFC is involved in the integration of sensory information and emotional stimuli. It contributes to the regulation of a variety of emotional and cognitive processes, including making decisions and guiding appropriate behavioral changes toward advantageous future outcomes [Bechara et al., 2000; Reuter et al., 2005]. Interestingly, the MPFC was also shown to mediate autonomic responses evoked by emotional stimuli, and lesions in the MPFC have been shown to compromise emotionally induced skin conductance or cardiovascular responses [Bechara et al., 2000]. Moreover, the MPFC and ACC exhibit top–down pain modulation during cognitive interference of nociceptive input [Bingel et al., 2007; Petrovic et al., 2002; Tracey and Mantyh, 2007; Wager et al., 2004]. This was demonstrated for placebo cognition [Bingel et al., 2006] and distraction from pain [Bantick et al., 2002; Valet et al., 2004]. The pain modulatory content seems to be mediated via brainstem nuclei like the PAG [Valet et al., 2004] which, along with the RVM, form the backbone of a descending pain modulatory system, projecting onto spinal dorsal horn neurons [Mason, 2005]. Furthermore, in the absence of cognitive interference the MPFC seems to be relevant for pain modulation [Derbyshire et al., 1997]. The DLPFC exerts active control on pain perception by modulating corticosubcortical and corticocortical pathways [Lorenz et al., 2003]. It can be speculated that these pain modulatory areas interfere with autonomic processing during the experience and anticipation of pain.

S2, Parietal Cortex, Cerebellum, and Motor Areas

In the present study and in previous studies S2 was activated during pain [Apkarian et al., 2005] and pain anticipation [Wise et al., 2007]. In our study activity in S2 correlated with SBF and SCR during pain experience and with SBF during pain anticipation. The parietal association cortex was also reported to be activated during pain [Seifert et al., 2010] and pain anticipation [Wise et al., 2007]. In the present study we found that parietal cortex activity correlated to SBF and SCR during pain experience and pain anticipation. Furthermore, ipsilateral activity in the thalamus correlated with SBF and SCR. This was more pronounced during pain experience than during pain anticipation. We detected cerebellar areas covarying with sympathetic activity. Cerebellar areas in which activity covaried with sympathetic activity were reported in previous studies involving exercise and mental stress [Critchley et al., 2000a] and decision making [Critchley et al., 2000b]. Also, the cerebellum is known to be activated in acute and chronic pain [Borsook et al., 2008; Moulton et al., 2010, 2011]. It was suggested that the cerebellum is involved in emotional and cognitive pain processing [Borsook et al., 2008]. The significance and role of the cerebellum in autonomic processing during pain must be evaluated in greater detail in future research. Last, correlations were observed in areas of the motor system (M1, SMA, PMC), temporal and occipital cortical regions and in the midbrain. If, as suggested by the present data, they play a role in cerebral autonomic processing, this role must be elucidated in future research.

A potential limitation of our study is that we cannot completely rule out the possibility that brain activity correlated with autonomic measurements could have been contaminated by brain activity induced by sensory or motor components of the pain sensation [Piche et al., 2010]. However, contamination with a sensory component of the painful stimulation can be excluded for the condition pain anticipation. Moreover, we tried to limit this problem by implementing two sympathetic parameters, SBF and SCR. A further limitation of the study is the small sample size. This has to be addressed explicitly as individuals vary substantially in their autonomic responses. It should also be mentioned that both male and female participants were used and may vary in their emotional reactivity. Furthermore, significant changes in sympathetic outflow during pain anticipation compared to innocuous warmth anticipation were detected for skin blood flow, but not for sympathetic skin response. This finding suggests that skin blood flow is the more sensitive parameter for sympathetic outflow in the present fMRI study. We noticed that, with the sampling rates (for example 1 kHz for SCR) and filters applied here, the laser-Doppler was less susceptible to scanner artifacts. However, this finding cannot be generalized as other sampling rates and filter settings may result in the opposite. Finally, it should be noted that we did not measure parameters associated with parasympathetic autonomic activity.

CONCLUSION

During the experience and anticipation of pain, activity in insular cortex, ACC, PFC, S2, parietal association cortex, thalamus, and midbrain correlated with parameters of sympathetic outflow. Thus, we have here described a shared central neural network associated with sympathetic responses to the experience and anticipation of pain.

REFERENCES

Apkarian AV, Bushnell MC, Treede RD, Zubieta JK (2005): Human brain mechanisms of pain perception and regulation in health and disease. Eur J Pain 9:463–484.

Bantick SJ, Wise RG, Ploghaus A, Clare S, Smith SM, Tracey I (2002): Imaging how attention modulates pain in humans using functional MRI. Brain 125(Part 2):310–319.

Bechara A, Tranel D, Damasio H (2000): Characterization of the decision-making deficit of patients with ventromedial prefrontal cortex lesions. Brain 123(Part 11):2189–2202.

Benarroch EE (2006): Pain-autonomic interactions. Neurol Sci 27(Suppl 2):S130–S133.

Bingel U, Lorenz J, Schoell E, Weiller C, Buchel C (2006): Mechanisms of placebo analgesia: rACC recruitment of a subcortical antinociceptive network. Pain 120:8–15.

Bingel U, Schoell E, Buchel C (2007): Imaging pain modulation in health and disease. Curr Opin Neurol 20:424–431.

Borsook D, Moulton EA, Tully S, Schmahmann JD, Becerra L (2008): Human cerebellar responses to brush and heat stimuli in healthy and neuropathic pain subjects. Cerebellum 7:252–272.

Brooks JC, Tracey I (2007): The insula: A multidimensional integration site for pain. Pain.

Buchel C, Morris J, Dolan RJ, Friston KJ (1998): Brain systems mediating aversive conditioning: An event-related fMRI study. Neuron 20:947–957.

Buchel C, Dolan RJ, Armony JL, Friston KJ (1999): Amygdala-hippocampal involvement in human aversive trace conditioning revealed through event-related functional magnetic resonance imaging. J Neurosci 19:10869–10876.

Chua P, Krams M, Toni I, Passingham R, Dolan R (1999): A functional anatomy of anticipatory anxiety. Neuroimage 9(6 Part 1): 563–571.

Colloca L, Benedetti F, Pollo A (2006): Repeatability of autonomic responses to pain anticipation and pain stimulation. Eur J Pain 10:659–665.

Craig AD (2002): How do you feel? Interoception: The sense of the physiological condition of the body. Nat Rev Neurosci 3:655–666.

Craig AD (2003): Interoception: The sense of the physiological condition of the body. Curr Opin Neurobiol 13:500–505.

Craig AD (2009): How do you feel now? The anterior insula and human awareness. Nat Rev Neurosci 10:59–70.

Craig AD, Chen K, Bandy D, Reiman EM (2000): Thermosensory activation of insular cortex. Nat Neurosci 3:184–190.

Critchley HD (2005): Neural mechanisms of autonomic, affective, and cognitive integration. J Comp Neurol 493:154–166.

Critchley HD (2009): Psychophysiology of neural, cognitive and affective integration: fMRI and autonomic indicants. Int J Psychophysiol 73:88–94.

Critchley HD, Corfield DR, Chandler MP, Mathias CJ, Dolan RJ (2000a): Cerebral correlates of autonomic cardiovascular arousal: A functional neuroimaging investigation in humans. J Physiol 523(Part 1):259–270.

Critchley HD, Elliott R, Mathias CJ, Dolan RJ (2000b) Neural activity relating to generation and representation of galvanic skin conductance responses: A functional magnetic resonance imaging study. J Neurosci 20:3033–3040.

Critchley HD, Mathias CJ, Dolan RJ (2001a) Neural activity in the human brain relating to uncertainty and arousal during anticipation. Neuron 29:537–545.

Critchley HD, Mathias CJ, Dolan RJ (2001b) Neuroanatomical basis for first- and second-order representations of bodily states. Nat Neurosci 4:207–212.

Critchley HD, Mathias CJ, Josephs O, O'Doherty J, Zanini S, Dewar BK, Cipolotti L, Shallice T, Dolan RJ (2003): Human cingulate cortex and autonomic control: Converging neuroimaging and clinical evidence. Brain 126(Part 10):2139–2152.

Critchley HD, Wiens S, Rotshtein P, Ohman A, Dolan RJ (2004): Neural systems supporting interoceptive awareness. Nat Neurosci 7:189–195.

Critchley HD, Tang J, Glaser D, Butterworth B, Dolan RJ (2005): Anterior cingulate activity during error and autonomic response. Neuroimage 27:885–895.

Derbyshire SW, Jones AK, Gyulai F, Clark S, Townsend D, Firestone LL (1997): Pain processing during three levels of noxious stimulation produces differential patterns of central activity. Pain 73:431–445.

Dube AA, Duquette M, Roy M, Lepore F, Duncan G, Rainville P (2009): Brain activity associated with the electrodermal reactivity to acute heat pain. Neuroimage 45:169–180.

Janig W, Habler HJ (2003): Neurophysiological analysis of target-related sympathetic pathways from animal to human: Similarities and differences. Acta Physiol Scand 177:255–274.

Leone M, Proietti Cecchini A, Mea E, Tullo V, Curone M, Bussone G (2006): Neuroimaging and pain: A window on the autonomic nervous system. Neurol Sci 27(Suppl 2):S134–S137.

Lorenz J, Minoshima S, Casey KL (2003): Keeping pain out of mind: The role of the dorsolateral prefrontal cortex in pain modulation. Brain 126(Part 5):1079–1091.

Maihofner C, Seifert F, Decol R (2010): Activation of central sympathetic networks during innocuous and noxious somatosensory stimulation. Neuroimage.

Mason P (2005): Ventromedial medulla: Pain modulation and beyond. J Comp Neurol 493:2–8.

Mobascher A, Brinkmeyer J, Warbrick T, Musso F, Wittsack HJ, Stoermer R, Saleh A, Schnitzler A, Winterer G (2009): Fluctuations in electrodermal activity reveal variations in single trial brain responses to painful laser stimuli–a fMRI/EEG study. Neuroimage 44:1081–1092.

Moulton EA, Schmahmann JD, Becerra L, Borsook D (2010): The cerebellum and pain: Passive integrator or active participator? Brain Res Rev 65:14–27.

Moulton EA, Elman I, Pendse G, Schmahmann J, Becerra L, Borsook D (2011): Aversion-related circuitry in the cerebellum: Responses to noxious heat and unpleasant images. J Neurosci 31:3795–3804.

Peltz E, Seifert F, Decol R, Dorfler A, Schwab S, Maihofner C (2010): Functional connectivity of the human insular cortex during noxious and innocuous thermal stimulation. Neuroimage 54:1324–1335.

Petrovic P, Kalso E, Petersson KM, Ingvar M (2002): Placebo and opioid analgesia—Imaging a shared neuronal network. Science 295:1737–1740.

Piche M, Arsenault M, Rainville P (2010): Dissection of perceptual, motor and autonomic components of brain activity evoked by noxious stimulation. Pain 149:453–462.

Ploghaus A, Tracey I, Gati JS, Clare S, Menon RS, Matthews PM, Rawlins JN (1999): Dissociating pain from its anticipation in the human brain. Science 284:1979–1981.

Ploghaus A, Narain C, Beckmann CF, Clare S, Bantick S, Wise R, Matthews PM, Rawlins JN, Tracey I (2001): Exacerbation of pain by anxiety is associated with activity in a hippocampal network. J Neurosci 21:9896–9903.

Porro CA, Baraldi P, Pagnoni G, Serafini M, Facchin P, Maieron M, Nichelli P (2002): Does anticipation of pain affect cortical nociceptive systems? J Neurosci 22:3206–3214.

Reuter J, Raedler T, Rose M, Hand I, Glascher J, Buchel C (2005): Pathological gambling is linked to reduced activation of the mesolimbic reward system. Nat Neurosci 8:147–148.

Saper CB (2002): The central autonomic nervous system: Conscious visceral perception and autonomic pattern generation. Annu Rev Neurosci 25:433–469.

Seifert F, Fuchs O, Nickel FT, Garcia M, Dorfler A, Schaller G, Kornhuber J, Sperling W, Maihofner C (2010): A functional magnetic resonance imaging navigated repetitive transcranial magnetic stimulation study of the posterior parietal cortex in normal pain and hyperalgesia. Neuroscience 170:670–677.

Seifert F, Maihofner C (2009): Central mechanisms of experimental and chronic neuropathic pain: Findings from functional imaging studies. Cell Mol Life Sci 66:375–390.

Shastri A, Lomarev MP, Nelson SJ, George MS, Holzwarth MR, Bohning DE (2001): A low-cost system for monitoring skin conductance during functional MRI. J Magn Reson Imaging 14:187–193.

Talairach J, Tournoux P (1988): Co-Planar Stereotaxic Atlas of the Human Brain. Thieme Medical Publishers. pp. 1–122.

Tracey I, Mantyh PW (2007): The cerebral signature for pain perception and its modulation. Neuron 55:377–391.

Treede RD, Kenshalo DR, Gracely RH, Jones AK (1999): The cortical representation of pain. Pain 79:105–111.

Tseng MT, Tseng WY, Chao CC, Lin HE, Hsieh ST (2010): Distinct and shared cerebral activations in processing innocuous versus noxious contact heat revealed by functional magnetic resonance imaging. Hum Brain Mapp 31:743–757.

Valet M, Sprenger T, Boecker H, Willoch F, Rummeny E, Conrad B, Erhard P, Tolle TR (2004): Distraction modulates connectivity of the cingulo-frontal cortex and the midbrain during pain—An fMRI analysis. Pain 109:399–408.

Wager TD, Rilling JK, Smith EE, Sokolik A, Casey KL, Davidson RJ, Kosslyn SM, Rose RM, Cohen JD (2004): Placebo-induced changes in FMRI in the anticipation and experience of pain. Science 303:1162–1167.

Wallin BG (1990): Neural control of human skin blood flow. J Auton Nerv Syst 30 Suppl:S185–S190.

Wasner G, Heckmann K, Maier C, Baron R (1999): Vascular abnormalities in acute reflex sympathetic dystrophy (CRPS I): Complete inhibition of sympathetic nerve activity with recovery. Arch Neurol 56:613–620.

Wise RG, Lujan BJ, Schweinhardt P, Peskett GD, Rogers R, Tracey I (2007): The anxiolytic effects of midazolam during anticipation to pain revealed using fMRI. Magn Reson Imaging 25:801–810.

Yarnitsky D, Sprecher E (1994): Thermal testing: Normative data and repeatability for various test algorithms. J Neurol Sci 125:39–45.